



Review

In flow-based technologies: A new paradigm for the synthesis and processing of covalent-organic frameworks

Pablo Martínez-Bulit^a, Alessandro Sorrenti^{a,b}, David Rodríguez San Miguel^a, Michele Mattera^a, Yonca Belce^a, Yanming Xia^c, Shenglin Ma^c, Mu-Hua Huang^d, Salvador Pané^e, Josep Puigmartí-Luis^{a,f,*}

^a Departament de Ciència dels Materials i Química Física, Institut de Química Teòrica i Computacional, University of Barcelona (UB), 08028 Barcelona, Spain

^b Departament de Química Inorgànica i Orgànica, University of Barcelona (UB), 08028 Barcelona, Spain

^c Department of Mechanical and Electrical Engineering, Xiamen University, Xiamen 361005, China

^d Experimental Center for Advanced Materials, School of Materials Science and Engineering, Beijing Institute of Technology, No. 5, Zhongguancun South Street, Beijing 100081, China

^e Multi-Scale Robotics Lab, ETH Zurich, Tannenstrasse 3, CH-8092 Zurich, Switzerland

^f Institució Catalana de Recerca i Estudis Avançats (ICREA), Pg. Lluís Companys 23, 08010 Barcelona, Spain

ARTICLE INFO

Keywords:

Microfluidic technologies
Crystallization
Covalent-organic frameworks
Reaction-diffusion mixing
Simulated microgravity

ABSTRACT

Nearly twenty years since the discovery of covalent-organic frameworks (COFs), most of the research on these materials has been focused on the rational design of new structures. Recently, the quest for discovering the functionalities and potential applications of these crystalline materials has attracted the attention of many researchers. While the number of reports regarding these two aspects within the COF research area is continuously growing, in order to achieve their full potential, the processability aspect of COFs also needs to be addressed. In this review article, we examine the opportunities that flow-based technologies offer regarding (a) the continuous synthesis of COFs, and (b) the processing of these materials into functional surfaces and devices (e.g. thin films and 3D structures), both aspects being ultimately amenable to industrial scale up.

1. Introduction

Covalent-organic frameworks (COFs) are a class of crystalline materials that form extended two-dimensional (2D) and three-dimensional (3D) porous structures by linking organic building blocks via reversible covalent bonds [1]. Despite all the knowledge gained in the synthesis of 2D and 3D COFs via reticular chemistry [2], the key parameters that govern their assembly and growth pathways are still poorly understood. For a new leap forward in the technological applications of COFs, the elucidation of the mechanisms directing the formation of COFs and the control over their morphogenesis are crucial [3,4]. These features are of paramount importance to control the properties and function of natural and new artificial matter [5].

To date, the main tool that researchers have used to control the bottom-up assembly of COFs is the rational design of their constituent building blocks [2,6]. In most COF syntheses, a series of bonding and unbonding events occur during the self-assembly process, ultimately yielding the most stable structure (the equilibrium state). To facilitate

the error-correction processes needed for the formation of these large extended structures, solvothermal synthesis conditions are normally used, along with the optimization of reaction parameters such as reactant and catalyst concentrations, and temperature [7]. Beside those classical approaches, another intriguing possibility to control COF synthesis is by harnessing the different self-assembly pathways that the system can follow while going from the initial non-assembled state to the final ordered structure, which is mostly overlooked in the COF research community [8–10]. Pathway complexity is intrinsic to extended supramolecular materials having complex, multi-well energy landscapes comprising several local minima of comparable stability (non-equilibrium states), along with the global minimum representing the thermodynamic product. If we can devise ways of steering the system in its journey across the free energy landscape, the level of control over its morphogenesis and final (supra)molecular structure can be greater. Underlying this possibility is the fact that: *i*) the self-assembly processes usually involve multiple competitive growth pathways featuring different kinetic mechanisms, and *ii*) the self-assembly occurs

* Corresponding author at: Departament de Ciència dels Materials i Química Física, Institut de Química Teòrica i Computacional, University of Barcelona (UB), 08028 Barcelona, Spain.

<https://doi.org/10.1016/j.cej.2022.135117>

Received 23 September 2021; Received in revised form 17 January 2022; Accepted 2 February 2022

Available online 5 February 2022

1385-8947/© 2022 The Author(s).

Published by Elsevier B.V. This is an open access article under the CC BY-NC-ND license

(<http://creativecommons.org/licenses/by-nc-nd/4.0/>).

in a far from homogeneous and constantly evolving environment, where concentration gradients and local inhomogeneities (e.g. solvent composition, pH gradients, temperature gradients) can have a markedly different impact on the various growth pathways.

Consequently, controlling the interaction of the assembling system with its surroundings in space and time (e.g. regulating the supply and mixing of reactants, chemical triggers, or catalysts) can enable an exquisite control over the size, shape, degree of defects, molecular packing, and associated functions of the artificial materials generated (*vide infra*). The source of inspiration for such level of control over reaction conditions comes from Nature, which masters reaction–diffusion (RD) processes to create intricate structures and patterns at different length-scales in both animate and inanimate matter, but also to control complex functions such as cell metabolisms, signalling, and gene expression in living systems [11]. To translate these concepts into a viable routine method for the preparation of artificial materials with targeted morphologies, properties, and functions, robust and versatile technologies that enable fine control over RD phenomena are needed. In this regard, microfluidic technologies are emerging as an extremely powerful toolkit for controlling self-assembly processes in the fields of both supramolecular polymers [10,12–14] and self-assembled materials [9,15–20]. It should be noted that while microfluidic devices have been extensively used as high-throughput screening platforms to optimise self-assembly and crystallisation processes as well as analytical tools to monitor crystal growth kinetics [21,22], the RD conditions achieved within a planar microfluidic device can offer much greater possibilities to unveil and control different self-assembly pathways during the synthesis of functional artificial matter in a given energy landscape [9,23]. Our group has been very active in this field, studying the effect of microfluidic RD conditions during the synthesis of coordination

polymers (CPs) and metal–organic frameworks (MOFs), both under continuous-flow and static conditions, *vide infra* [13,23–25]. Relevant review papers are available in the literature, addressing the application of microfluidic technologies to the synthesis of MOFs and other porous materials such as zeolites [9,26–28]. In this review, we will instead focus on the applications of in-flow based technologies for COFs synthesis, which is a nascent but highly promising research field. We believe that discussing the current corpus of works on this topic, with a specific focus on the physical properties that different microfluidic technologies can (or cannot) allow to control, will help to lay the foundations for future developments, motivating further applications of microfluidic technologies in the COFs synthesis domain.

Continuous-flow microfluidic devices operating under laminar flow conditions can enable the mixing of the chemical species dissolved in co-flowing streams solely via molecular diffusion [29,30]. This condition allows for an exquisite spatiotemporal control of self-assembly events (e.g. encounter of the assembling species at the liquid–liquid interface) and of the surrounding medium (e.g. regulation of concentration gradients joined with a constant mass transport of reactants to the RD area), which in turn allows for pathway selection (see Fig. 1) [9]. In sharp contrast, conventional bulk synthetic methods characterised by chaotic turbulent mixing, or segmented-flow microfluidic approaches (droplet-based methods), do not provide any comparable degree of control over RD processes (Fig. 1 and Table 1), *vide infra*.

We have demonstrated that continuous flow microfluidic devices operating under laminar flow conditions can: *i*) change the π - π stacking distance of a conductive supramolecular aggregate by simply controlling the flow focussing conditions; [31] *ii*) modify the morphogenesis of CPs during their in-flow self-assembly; [24] *iii*) isolate early intermediate states of a CP along a single crystallisation pathway; [13] *iv*) engineer

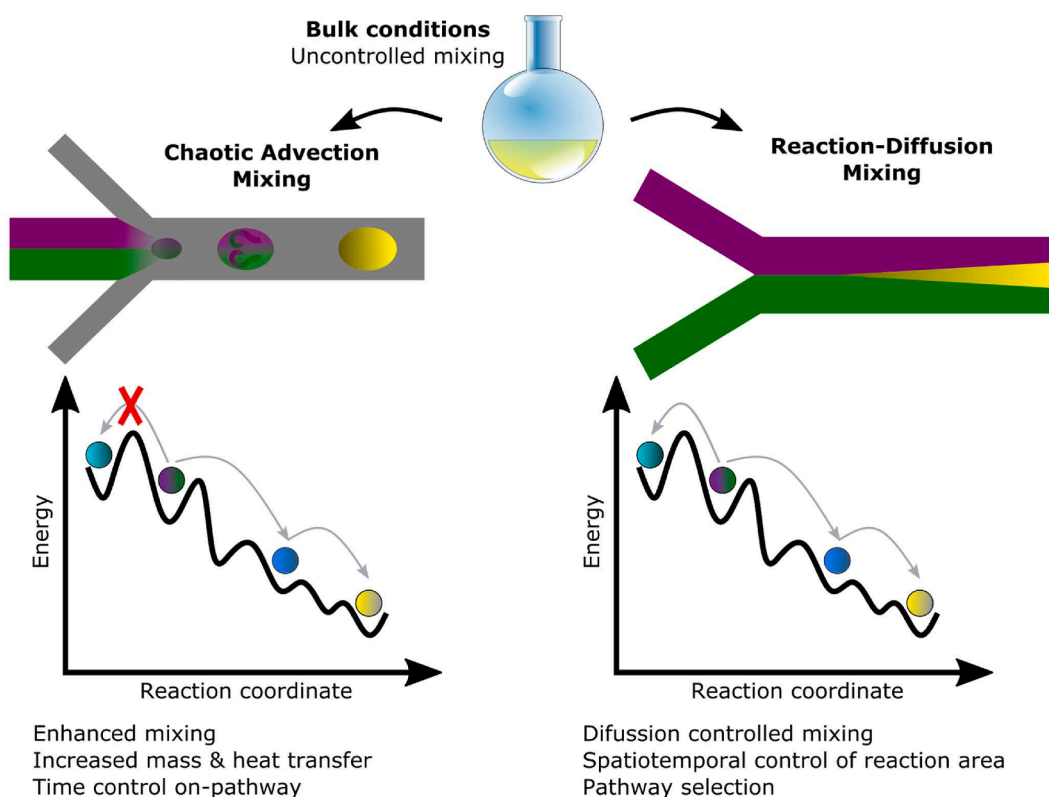


Fig. 1. Schematic illustrations comparing the mixing of reagents in a round-bottom flask (bulk mixing) with both a segmented-flow method, and a continuous microfluidic mixing approach. While turbulent mixing is commonly used in bulk synthetic approaches, different mixing regimes can emerge with segmented and continuous-flow microfluidic devices. Segmented flow offers a much faster mixing but the only factor that can be controlled is the droplet residence time in the reactor. Continuous microfluidic mixing approaches allow for the spatiotemporal control of reagent diffusion, thus making pathway selection possible. In all cases it is possible to reach the thermodynamic product.

Table 1
Comparison between different synthetic approaches used for the synthesis of COF materials.

		Physical properties	Advantages	Drawbacks
Bulk synthesis		<ul style="list-style-type: none"> - Uncontrolled turbulent mixing - Gravity - Low surface area to volume ratio 	<ul style="list-style-type: none"> - Easy to operate - Straightforward scaling-up - <i>In situ</i> characterization is possible 	<ul style="list-style-type: none"> - Requires solvothermal conditions - Poor level of control on the formed material - Unprocessable powders - Higher consumption of reagents - Small working volumes - Scaling-up may require parallelization - Potential issues with clogging, optimization is always required
Microfluidic synthesis	Co-flowing streams	<ul style="list-style-type: none"> - Low Reynolds numbers - Purely diffusive mixing. - Spatiotemporal control of the reaction zone and chemical gradients - Little gravity effect - High surface area to volume ratio 	<ul style="list-style-type: none"> - Isolation of kinetic products - Pathway selection - Mechanistic insight - Material processability (fabrication of films and 3D printed structures) - <i>In situ</i> characterization is possible - Excellent manipulation of reagents 	
	Segmented flow (droplet microfluidics)	<ul style="list-style-type: none"> - Chaotic advection mixing - Enhanced mass and heat transfer - High surface area to volume ratio 	<ul style="list-style-type: none"> - Accelerated synthesis and improved yields - In-line post-synthetic modification - Core-shell composite synthesis - <i>In situ</i> characterization is possible - Excellent manipulation of reagents - Simultaneous screening analysis, <i>i.e.</i> high-throughput data acquisition 	<ul style="list-style-type: none"> - Uncontrolled RD mixing - Contamination of the products with the carrier phase - Poor processability
	Static microgravity mimicking conditions	<ul style="list-style-type: none"> - Low Grashof numbers - Advection free mixing - Defined concentration gradients - Little gravity effect - High surface area to volume ratio 	<ul style="list-style-type: none"> - Production of large, defect-free films - <i>In situ</i> characterization is possible - Excellent manipulation of reagents 	<ul style="list-style-type: none"> - Requires custom-made reactors - Early stage of development

defects in the crystal structure of a well-known and robust spin-crossover (SCO) complex, which resulted in an unprecedented change of its spin transition behaviour; [32] and v) unveil unprecedented growth pathways during the synthesis of a MOF [23].

As for microfluidic devices in static conditions, the physical properties of these reaction environments can also be favourably exploited. Submicrolitre spaces are characterised by low Grashof numbers, at which viscous forces dominate over buoyancy forces, resulting in the absence of advection currents [33]. These conditions closely resemble those occurring in the outer Space, *i.e.* under microgravity conditions [34]. We showed that performing crystallizations in these microgravity-mimicking environments can enable control over crystal morphogenesis. Specifically, our group demonstrated that it is possible to avoid the typical polyhedral shape of MOF crystals and achieve millimetre-sized single crystals of a peptide-based MOF with intricate morphologies, including crystals with curved faces [25]. Such morphologies arise from the interplay between the diffusion-controlled mixing of the precursors in an advection-free environment and the physical constraints (barriers) imposed during crystal growth, mimicking the two main strategies of morphogenesis in biomineralisation [35].

Considering that the control over size and shape of porous materials, and their facile processability, are key requirements for their successful implementation into functional devices, translating the strategies already implemented by our group and others into the field of COFs can promote their real-life applications [15,36]. In the following sections, we highlight the different approaches that have been used so far to synthesise COFs taking advantage of the unique synthetic conditions provided by microfluidic-based technologies.

2. Synthesis under continuous flow

As described in the introduction, the use of continuous-flow microfluidic methods can be advantageous when the goal is to achieve a spatiotemporal control over self-assembly processes. This control during the mixing of reagents can lead to new mechanistic insights into crystallisation events, enabling the isolation of unprecedented and earlier intermediate states [13] or unveiling new crystallisation pathways [23]. Furthermore, continuous-flow microfluidic devices can also be valuable

tools to improve the processability of the materials generated, and to increase their yield-over-time. Note that all these features can provide useful additional information for the controlled morphogenesis of COFs as well as their scaled-up synthesis in an industrial setting.

Continuous-flow microfluidic methods include both droplet-based approaches, *i.e.* segmented flows, and continuous-flow methods based on co-flowing streams. While in the case of droplet-based methods chaotic advection mixing dominates without any possible control on RD phenomena, in the case of planar continuous-flow devices operating with co-flowing streams, an exquisite control over RD mixing is established (Fig. 1) [30].

In this section, different examples of the application of continuous-flow microfluidic methods for the preparation of COFs have been grouped based on the physical mixing regime in which they are obtained, either controlled RD mixing or chaotic advection mixing.

2.1. RD mixing: Mixing via a controlled diffusion of precursors inside a microfluidic device

The first report showing the synthesis of a COF employing a continuous-flow microfluidic device was published by Puigmartí and co-workers in 2016 [37]. A planar four-inlet device made of poly(dimethyl) siloxane (PDMS) was used to establish controlled RD mixing of the reactants (Fig. 2a). Specifically, solutions of the precursors 1,3,5-tris(4-aminophenyl)benzene (TAPB) and 1,3,5-benzene(tricarbaldehyde) (BTCA) were injected through the inner inlets of the device (B and C in Fig. 2a), generating co-flowing streams, while two sheath flows of glacial acetic acid were pumped through the external inlets (A and D in Fig. 2a). Due to the laminar flow conditions in the main microchannel (low Reynolds number), the reactants mixed solely via molecular diffusion. The sheath flows, in turn, allowed to tune the RD area during the synthesis of the COF (by flow focussing), and to prevent clogging of the device, while providing a constant supply of protons needed to ensure the reversibility of the covalent interactions during the synthesis of the COF.

With this experimental setup, the synthesis of the so-called **MF-COF-1** (microfluidic COF-1) could be performed in a timeframe of milliseconds, at room temperature and standard pressure. Moreover, **MF-COF-1**

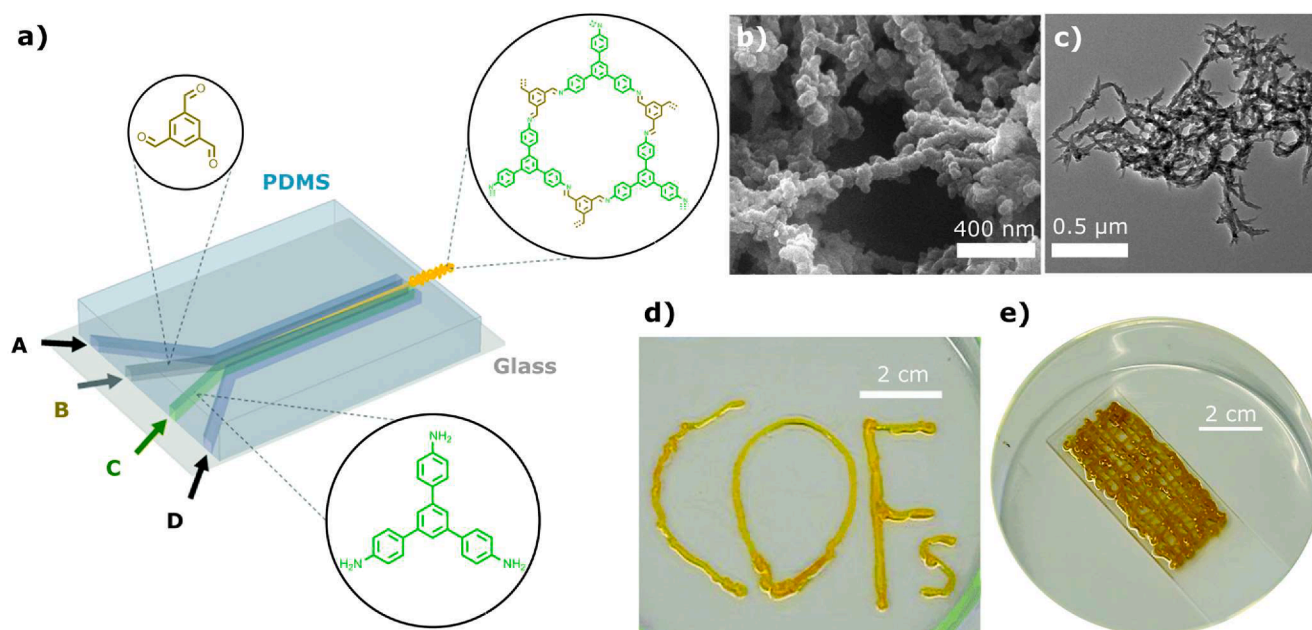


Fig. 2. Experimental setup for the synthesis of MF-COF-1 using a planar microfluidic device. a) 4-inlet microfluidic PDMS device (main channel 1 cm long, 250 μm wide, and 50 μm high). b) Field Emission SEM image of MF-COF-1. c) SEM image of MF-COF-1 fibres. d and e) printed macroscopic fibres of MF-COF-1 deposited on glass substrates. Adapted from [37] with permission from the Royal Society of Chemistry.

was collected at the outlet in the form of crystalline macroscopic fibres (Fig. 2d). The bulk synthesis of the same COF using turbulent mixing results in the formation of a gel. After washing and annealing the gel, scanning electron microscopy (SEM) analysis shows a particle size distribution of 60 nm and no further ordering of these particles into superstructures. On the other hand, analysis of MF-COF-1 by SEM showed a sponge-like structure made of meshes of MF-COF-1 nanofibres (Fig. 2b, c). These nanofibres are in turn made by the linear aggregation of nanoparticles of ca. 40 nm in size (Fig. 2b). The assembly of these structures can be rationalised as resulting from the narrow area where the building blocks mix, which forces an anisotropic aggregation of the crystallites. Remarkably, the authors demonstrated that the continuous flow microfluidic synthesis of MF-COF-1 can be used to directly print the material in 2D and 3D structures (Fig. 2d and 2e, respectively) [38]. This result was of great importance in the field, as for the first time it was demonstrated that COFs could be processed directly from the liquid phase as well as deposited on multiple surfaces to generate intricate printed structures. Even though the morphology and processability of MF-COF-1 was improved in this continuous-flow synthesis, the experiments performed did not offer new insights into the mechanisms underlying the COF formation.

Shortly after the work by Puigmartí and co-workers, Zhao and colleagues demonstrated that COFs can also be generated inside a polytetrafluoroethylene (PTFE) coiled tubing reactor employing a continuous-flow system [39]. Under these operating conditions, the reactant-laden fluids do not merely mix via RD conditions, but mass transport by advection can also occur. In fact, the coiled shape of the reactor can promote the formation of secondary flows (Dean vortices) perpendicularly to the flow along the main channel. Accordingly, significantly more complex fluid flow phenomena can emerge within a coiled tube than in a planar continuous-flow microfluidic device, which can lead to poorly controllable RD conditions [40]. Nonetheless, the authors demonstrated that their approach can be a simple option to scale up COF production under mild conditions.

Specifically, COF-LZU1, an imine-linked COF generated from the reaction of 1,3,5-triformylbenzene (TFB) with *p*-phenylenediamine (PDA) was chosen as the best-case scenario to demonstrate their continuous-flow synthetic method (Fig. 3). A T-junction setup was used

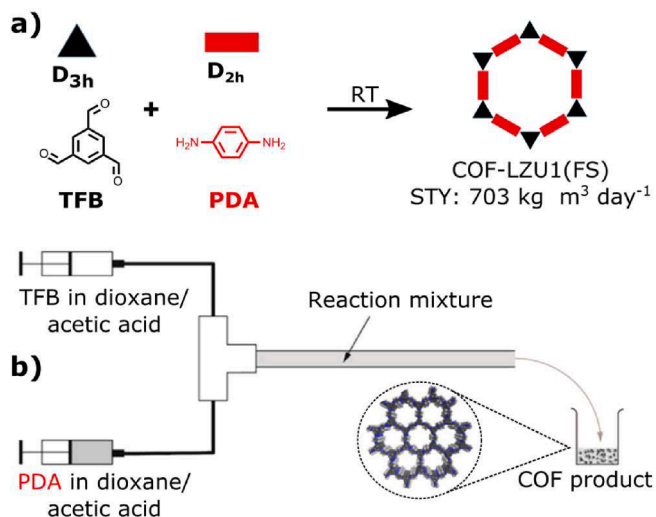


Fig. 3. Synthesis of COF-LZU1 in a continuous flow setup. a) Building blocks used for the synthesis of COF-LZU1 with their respective point group symmetry. b) schematic illustration of the T-micromixer setup used for the synthesis of COF-LZU1. FS stands for flow synthesis. Adapted with permission from [39]. Copyright © 2016 American Chemical Society.

to put into contact and mix the streams of the reactants TFB and PDA, see Fig. 3b. The COF crystallites were formed after an overall residence time of 11 s in the coiled tubing reactor. The quality of COF-LZU1 generated through this methodology was comparable to that obtained using analogous bulk conditions (and longer reaction times), but with a small increase in the Brunauer-Emmett-Teller (BET) surface area. When comparing this report with the conditions required to form MF-COF-1, the main difference is the reactor length and the residence times required to form the COFs. While Puigmartí and co-workers reported yields of almost 2 mg of MF-COF-1 per minute [37], this method produces about 0.7 mg of COF-LZU1 per minute. In this same work, Zhao and co-workers also synthesised three other COFs using a solution-suspension approach (SSA), but only one of these COFs could be

efficiently prepared under flow conditions. The latter clearly indicates that finding the right conditions for solubilising the COF precursors but also allowing for the fast formation of COF materials inside a microfluidic setting is a challenge that requires further knowledge of the mechanisms that favour the formation of their crystalline phases instead of their amorphous intermediates.

To sum up, these two papers demonstrate that it is possible to generate COFs employing continuous flow processes flexible for the scaling-up required for commercial production. As we expand the available examples of materials obtained by continuous flow approaches, the development of technologies for the industrial production of COFs will have a better chance at succeeding.

Continuous-flow approaches have been also used to directly integrate 2D COFs onto surfaces. Typically, the method used to grow 2D COFs onto a desired surface involves the immersion of a surface inside the reaction media and allowing the reaction to proceed normally. As a result, in many solvent mixtures and with a variety of surfaces, the COF will grow both in the bulk of the solution and on the immersed surface, generating a film on it. However, this bulk approach presents several disadvantages arising from depletion of the reaction mixture during the synthesis process. In addition, over time, the particle size of the COF crystals being produced changes, resulting in inhomogeneous or contaminated films. Finally, and more importantly, the control over the thickness of the deposited films is severely limited in this bulk synthesis. Since there is a minimum reaction time needed for the COF to become a crystalline material, very low thicknesses are limited to the minimum ripening time of the COF particles. Additionally, the maximum achievable thickness is also limited by the concentration of precursors since, once they deplete, the film can no longer grow. Thus, the concentration ranges that can be used for this approach has to be kept within certain limits that might not be straightforwardly determined. The use of a continuous-flow system can circumvent all these limitations, since at any given spatial point inside the device, the concentrations and reaction times are always constant. Capitalizing on this capability, Dichtel and colleagues reported the synthesis of highly uniform boronate ester-linked COF thin-films inside a commercially available quartz crystal microbalance (QCM) system equipped with a continuous flow cell accessory (Fig. 4) [41]. A reaction mixture composed of the two COF precursors was passed through a heat reservoir and then fed inside the continuous-flow device (Fig. 4a), which allowed for continuously and uniformly growing four different boronate-ester COF films with thicknesses higher than those that are attainable by the bulk approach.

Although this continuous-flow synthesis does not provide spatiotemporal control over the mixing of precursors, the flow device incorporated a QCM substrate that enabled the monitoring of the mass deposited during film growth. This proved to be a remarkably useful setup to gain new mechanistic insights on the crystallisation process of these materials. For example, the authors demonstrated that crystalline boronate-ester-linked COF films were only generated when longer residence times were used (Fig. 4c). This result indicates that oligomeric and polymeric species may play a key role during the film formation of these COF materials.

2.2. Chaotic advection mixing: Mixing of precursors inside a microfluidically generated droplet

If, instead of using a continuous flow microfluidic device with co-flowing streams, a segmented-flow microfluidic method is employed during the synthesis of a COF, the mixing of the COF precursors will change from a diffusion controlled regime to a chaotic advection mixing (Fig. 5c) [29]. In sharp contrast to the spatiotemporal control mixing achieved inside a planar continuous-flow microfluidic device operating under RD conditions, the reaction time in a chaotic advection mixing will be determined by the distance that the reagents inside the droplets travel throughout the microfluidic device [29]. That is, in a chaotic advection mixing regime the diffusion of the reagents (*i.e.* inside the droplet) cannot be controlled by simply changing the reagents flow rates [29]. Additionally, the stick-slip motion of the droplets will also play a role in the uncontrolled mixing of reagents [43].

In 2018, Kim and co-workers reported for the first time the synthesis of three different β -ketoenamine-linked COFs employing a segmented-flow microfluidic method (Fig. 5), namely **TpPa-H**, **TpPa-Me** and **TpPa-NO₂** (where Tp stands for 1,3,5-triformylphloroglucinol and Pa-H, Pa-Me and Pa-NO₂ for 1,4-phenylenediamine, 2,5-dimethyl-1,4-phenylenediamine and 2-nitro-1,4-phenylenediamine, respectively) [42]. The droplet-based generator was fabricated connecting transparent PTFE tubing to a T-junction, see Fig. 5. The authors used silicone oil as the continuous phase and a partially solubilised mixture of precursors in acidic media as the discontinuous phase. The immiscibility between the continuous and discontinuous phase enabled a facile droplet generation at the T-junction, where the two flows converge. Once generated, the droplets were directed to a coiled PTFE section of the device that was immersed in an oil bath. The authors optimised the microfluidic synthetic approach and found that **TpPa-H**, **TpPa-Me**, and **TpPa-NO₂**

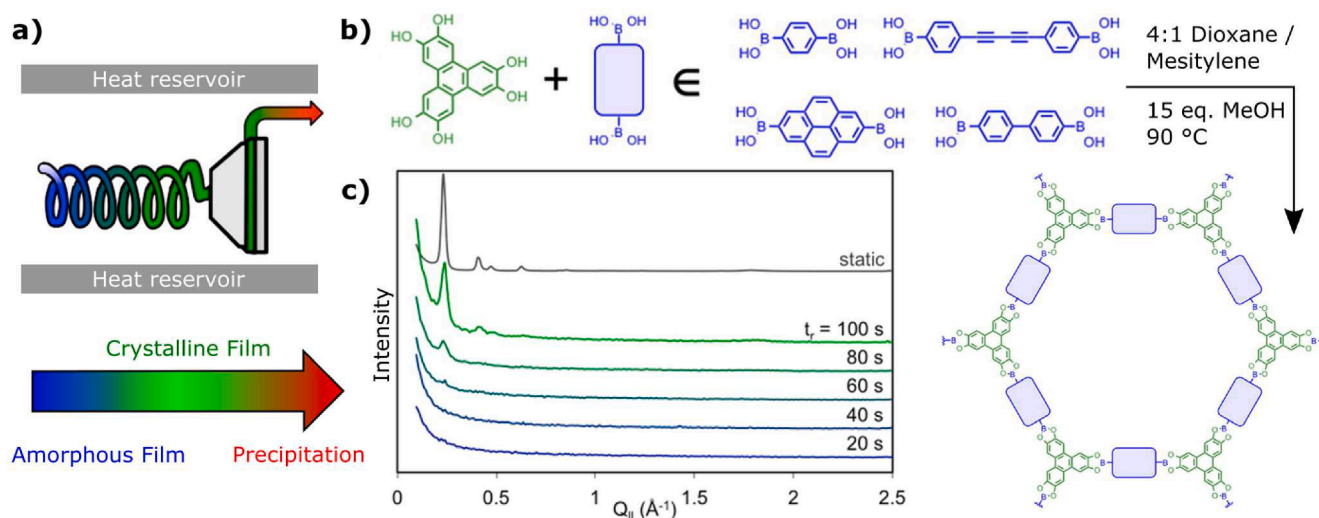


Fig. 4. Synthesis of boronate-ester COFs in a continuous-flow setup. a) Diagram showing the heat reservoir, the flow reactor, and the quartz microbalance where COF films grow, b) organic building blocks employed, c) ex situ grazing incidence X-ray diffraction (GI-XRD) patterns showing the increase of crystallinity of the COF films over time. Adapted with permission from [41]. Copyright © 2016 American Chemical Society.

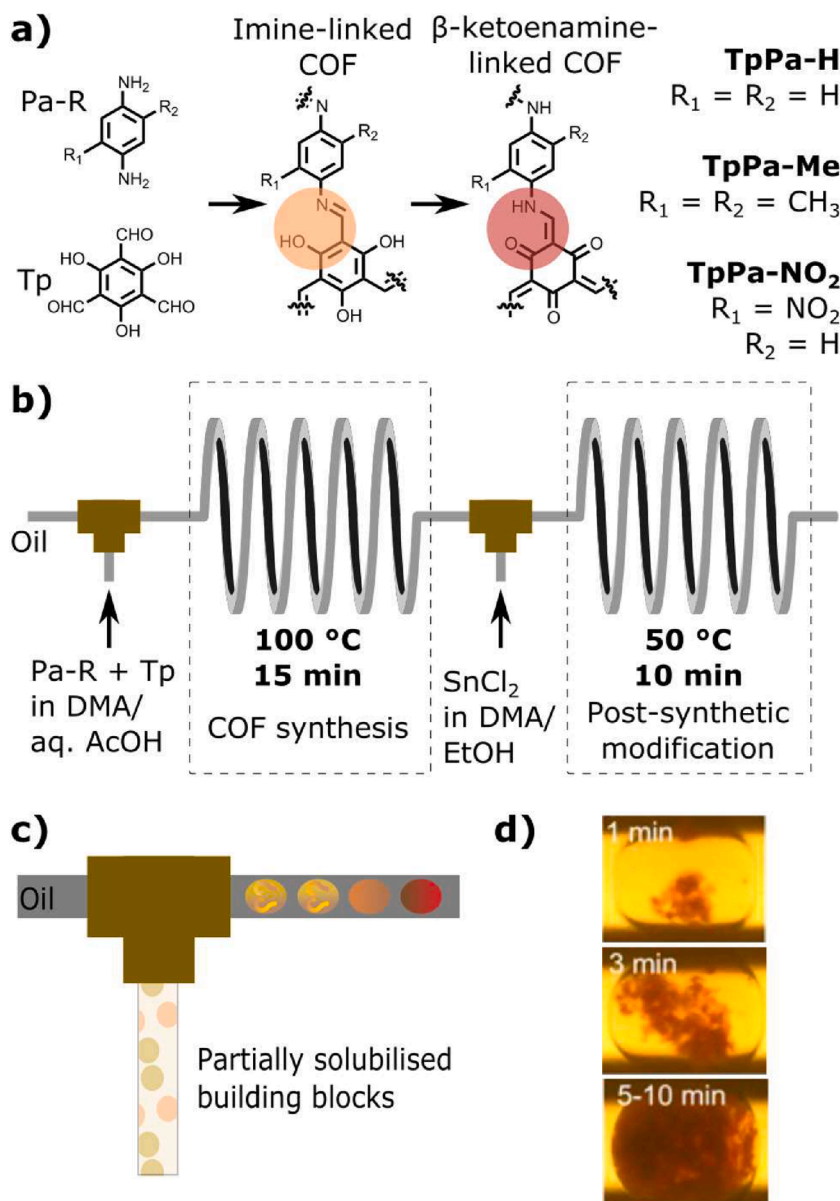


Fig. 5. Experimental setup used for the segmented-flow synthesis of TpPa-based COFs. a) Molecular structure of the building blocks and resulting COFs. b) Schematic illustration of the segmented-flow reactor showing the first T-junction used for COF synthesis and the second one used for the subsequent post-synthetic modification. c) Simplified scheme showing the chaotic mixing inside the droplets and the progression of the reaction. d) Optical microscope images of the droplets at different time scales during the synthesis of the TpPa-based COFs. Adapted with permission from [42]. Copyright © CC BY 4.0.

exhibited a higher degree of crystallinity, compared to the same materials synthesised in bulk conditions, when the residence time was set at 15 min and the reactor temperature at 100 °C. One drawback of β -ketoenamine COFs is that the tautomerisation step is irreversible, resulting in a poor self-correction process, and hence, in a low probability of enhancing the degree of crystallinity in the yielded products regardless of the synthetic method employed. After the COFs are formed inside the droplets, the authors showed that using the same microfluidic device in series, it is possible to subsequently modify the COF materials eliminating time-consuming separation and purification steps. For example, it was demonstrated that this serial microfluidic method could efficiently reduce the nitro substituents present in **TpPa-NO₂** into their aniline counterparts, producing **TpPa-NH₂** via an in-line post-synthetic modification (Fig. 5). While this work demonstrates a way to produce various COF powders, and an accessible method to introduce valuable functional groups via an in-line microfluidic post-synthetic modification, COF syntheses in which the precursors are partially soluble are problematic for a continuous flow setup. Such insolubility can easily clog the flow reactors, and the stoichiometric mixing of suspensions cannot be accurately controlled. Although the use of segmented-flow

microfluidic methods is a viable way to produce and post-modify COFs in a continuous manner, the formation of films of these materials, with controlled thicknesses and dimensions, would facilitate their incorporation into functional devices. Accordingly, it is highly necessary to develop new technologies that can facilitate the direct integration of COFs onto different surfaces, while still controlling the diffusion of reagents (e.g. minimising the natural convection flows) and avoiding uncontrolled precipitation. These technologies could undoubtedly accelerate the implementation of COF materials in emerging devices, and more importantly, in products with a socio-economic impact.

3. Synthesis under static conditions: Mimicking microgravity

Recently, it has been shown that static microfluidic conditions can lead to a controlled formation of a desired crystal habit during the synthesis of a MOF [25]. For example, 2D MOF crystals have been grown on a surface controlling the diffusion of MOF precursors in a simulated microgravity environment accomplished inside a microfluidic device [25]. Note that under these simulated microgravity conditions the usual polyhedral shape of MOF crystals can be suppressed, and new crystal

habits are available, where their thicknesses and dimensions are within easy reach.

Since the '80s [44], the space environment – where buoyancy-induced convective transport is absent – [45] has been considered a “dream playground” for the development of highly ordered materials. In fact, the convection-free mass transport, which exists in microgravity conditions, can greatly favour the synthesis of materials with larger crystalline domain sizes, lower defect densities and new morphologies [46]. Several studies have demonstrated that microgravity conditions can be exploited to favour the formation of single crystals [47,48], glasses and fibres [49,50], and other defect-free 3D materials [51–54]. Since 2010, several companies have been experimenting at the International Space Station's (ISS) U.S. National Laboratory, as microgravity is thought to be the ideal condition to achieve ground-breaking advances in the engineering of new functional materials and devices. However, the high costs and restricted access associated with experimentation in space is hindering further progress in this exciting field.

As discussed above, one way to simulate the microgravity conditions present at the International Space Station is by confining reactions to small spaces and working with very low volumes. To this extent, a recent study by Sotto Mayor, Ruiz-Molina, and Puigmartí showed how to apply

this approach to the synthesis of COF films and other porous 2D materials [55]. By using a custom-made microfluidic device (Fig. 6a and b), the authors could achieve a buoyancy- and convection-free environment. Numerical simulations showed that the mass transport inside these microfluidic devices occurs without the presence of vortices (Fig. 6d), in sharp contrast to what occurs in a typical vapour-assisted conversion (Fig. 6c). The experimental setup also allows for the diffusion of gases with a vertical concentration front (*i.e.* perpendicular the Earth gravity), translating in the formation of more homogeneous films (Fig. 6e). The confined space in which the reaction takes place, and the unique mass transport regime inside the microfluidic device, promotes the growth of crack-free, compact and centimeter-sized thin films onto different surfaces (Fig. 6e and f). Explicitly, they demonstrated a method to obtain thin films of COF-TAPB-BTCA with thicknesses as low as 60 nm (Fig. 6h and i). Characterisation data showed the characteristic XRD peaks of COF-TAPB-BTCA, with a preferential orientation of the film. Indeed, atomic force microscopy (AFM) and SEM measurements indicate that the defect-free centimetre-sized COF-TAPB-BTCA films have an extremely low roughness (RMS = 2.4 nm). Note that using the same reactions conditions in a bulk synthetic approach only COF-TAPB-BTCA particles are generated (Fig. 6g). This result clearly confirms that

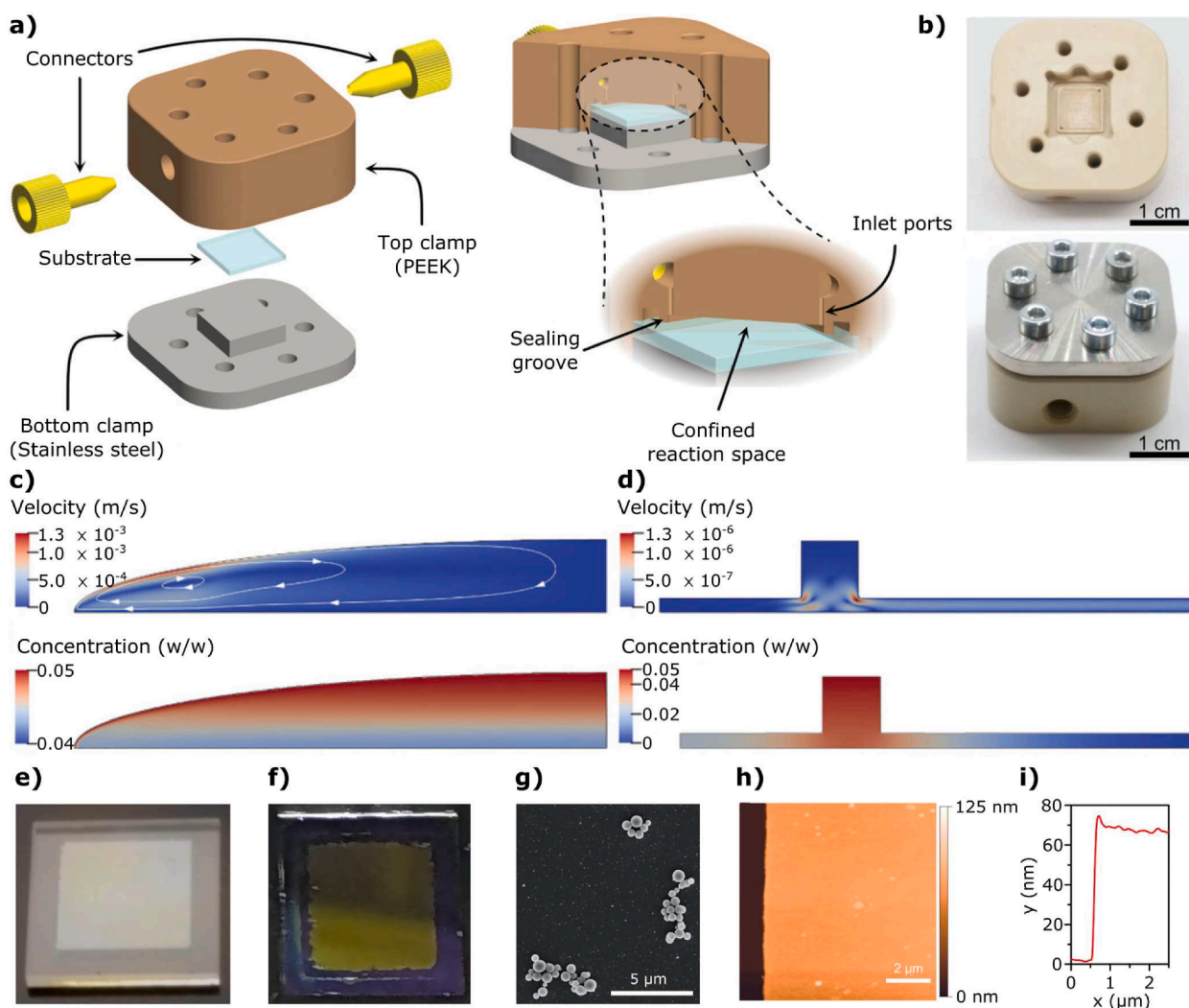


Fig. 6. Synthesis of COF-TAPB-BTC under microgravity conditions. a) Schematic illustration of the custom-made microfluidic device fabricated to simulate microgravity conditions on Earth, b) photographs of the confined reaction space and assembled microfluidic device. c) numerical simulations of the flows in a droplet showing convective currents and a concentration gradient parallel to the gravitational field. d) numerical simulations of the flow in the microfluidic device showing a concentration gradient perpendicular to the gravitational field. e and f) optical photographs of COF thin films on 1×1 cm quartz (001) and graphene, respectively. g) SEM image of COF-TAPB-BTC particles generated in bulk. h) AFM image of the edge of a COF-TAPB-BTC film on a quartz (001) substrate and i) height profile of the COF thin film. Adapted from [55] with permission from Wiley-VCH Verlag GmbH & Co. Copyright © 2021.

simulated microgravity can play a key role to control morphogenesis in COF synthesis. An additional annealing step was necessary to promote the crystallisation of the film, making the streamlining of the synthesis in an industrial setup a complicated step that requires further optimisation before scale-up is considered. However, this research area is still in its infancy and further research and technical developments are necessary in the future for a broad take-up by the scientific community as well as the industrial sector.

4. Post-synthetic processing of COF materials with microfluidic devices and under continuous flow

The control over the shape, localization, and integration of COFs with other components of a functional device is key to enable a future uptake of these materials by technological industries. However, their inherent insolubility once synthesised and the highly energetic synthetic conditions pose a challenge that has not been fully solved yet [36]. The higher control of mixing, diffusion, and temperature gradients in microfluidic devices is a great tool to advance in this endeavor. As such, some of the methods explained above tackle these limitations and allow for processing COFs during their formation, e.g. flow systems can be used to print fibers or to grow thin films. However, microfluidic systems can also process already formed COFs, as we will explain in the following section.

An example of how microfluidic devices can be used for processing COFs after they have been synthesised was recently reported by Puigmartí and co-workers. In this work, the authors take advantage of cationic micellar systems to generate printable COFs [56]. The aqueous micellar system was formed by cationic hexadecyltrimethylammonium bromide (CTAB) and anionic sodium dodecyl sulfate (SDS) surfactants in a 97:3 ratio, respectively (Fig. 7a). This ratio is important to form small mixed micelles instead of larger vesicles and hence to fine control the reaction outcome. When mixing TAPB and BTCA, each one solubilised in the CTAB/SDS mixture in water, in the presence of acetic acid, a stable colloidal orange solution was formed (Fig. 7b). The colour is indicative of the presence of imine bonds, and the average particle size of the COF was 16 nm. Extended small-angle X-ray scattering (SAXS) studies revealed the kinetics of the formation of these particles, which evolve from a TAPB-BTCA-COF single stack disk to a ten layered stack surrounded by the surfactants over 21 h. The COF particles could be isolated by inducing precipitation with ethanol, and upon further characterisation it was confirmed that they are crystalline. A second COF system was produced with the same methodology, i.e. Tz-COF, obtained from the reaction of 2,4,6-tris(4-aminophenyl)-1,3,5-triazine and BTCA. The homogeneous nature of these COF colloids and their behaviour upon ethanol addition enabled a controlled aggregation of the COF particles using the right tools. As a first example, when the reaction mixture after ethanol addition was inserted into a customised micro-clamp (Fig. 7c), free standing films were obtained after solvent evaporation, with a thickness between 0.5 and 50 μm (Fig. 7d). More interestingly, the injection of the micellar solution inside a 3D flow-focusing microfluidic device (Fig. 7e) allowed to finely control the mixing with ethanol, resulting in the direct printing of TAPB-BTCA-COF fibres over a variety of surfaces (Fig. 7f). As shown, this method is highly versatile and can generate processable COF inks that can be transformed into pure COF structures, hinting towards the importance of flow technologies in the shaping of COFs, particularly to achieve hierarchical 3D printed COF architectures. Even though this methodology is still in need of significant development, the ability to print COFs makes it extremely promising, since the 3D printing of hierarchical architectures with bare COFs is a milestone that has not been achieved yet. The few existing reports, even though at a more advanced stage of development, need a matrix (Pluronic F127 or graphene oxide) to support the printing of 2D COFs into three-dimensional shapes [57,58].

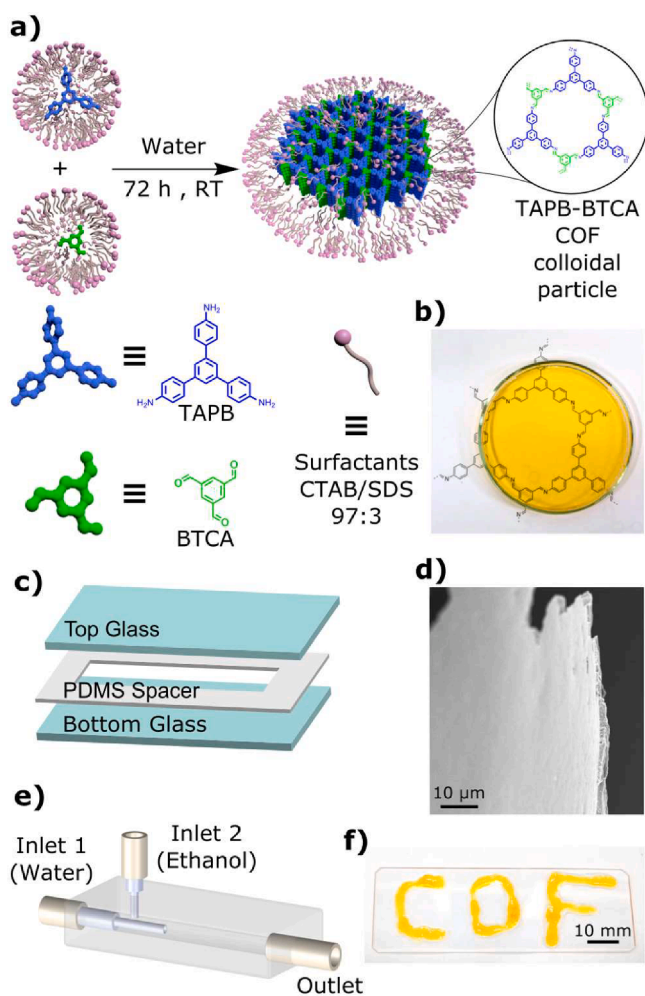


Fig. 7. Cationic micellar synthesis of COF-TAPB-BTCA. a) Organic building blocks and synthetic conditions used for the obtention of colloidal COF-TAPB-BTCA particles. b) Photograph of a transparent colloidal solution of COF-TAPB-BTCA. c) schematic illustration of the microfluidic clamp for the fabrication of COF-TAPB-BTCA films. d) SEM cross-section image of a COF-TAPB-BTCA film. e) schematic illustration of the microfluidic 3D flow-focusing device used for the direct printing of COF-TAPB-BTCA. f) macroscopic structure of printed COF-TAPB-BTCA fibres over a glass substrate. Adapted with permission from [56]. Copyright © 2020 American Chemical Society.

5. Summary and outlook

In this review, we have introduced microfluidic devices as a tool technology to synthesise and process COFs. The main advantages of this approach are directly related with the physical phenomena that can be controlled when working under microfluidic regimes. For example, if the mixing of COF precursors is enhanced by restricting the reaction volume to a droplet, i.e. in a segmented-flow approach, shorter synthesis times can be used and the heat and mass transfer during the reaction are increased. With this approach, the synthesis of COF powders can be improved to produce materials in large volumes over time, see Table 1.

When the building blocks are combined under RD conditions, the spatiotemporal control of the reaction can have various outcomes: i) the reaction time can be drastically reduced and the continuous formation of COFs can result in increased yields over time when compared to batch synthesis; ii) it is possible to directly generate COF materials in the form of crystalline fibers without further processing steps needed; and iii) relevant information about reaction mechanism and crystallite morphogenesis could also be obtained, see Table 1.

Alternatively, it has been demonstrated that by working under

microfluidic static conditions it is possible to simulate microgravity, a scenario that enables the formation of large, smooth, and crack-free COF thin films. These results showcase how both continuous flow and static microfluidic conditions can be employed to synthesise and process COFs. However, despite the advantages, there are aspects in the use of microfluidic devices for the synthesis of COFs that need further development and optimisation. We believe that focusing on the following points can further impulse the advancement of this field:

i) Understanding the nucleation and crystal growth events occurring during the self-assembly of COFs can provide information on how to adjust the synthetic protocols for targeted morphologies, properties, and functions in these materials. In this context, experiments performed in confined spaces such as in micelles, RD areas or simulated microgravity environments can provide valuable information. Likewise, expanding the scope of flow-based synthesis to study crystallisation events of 3D COFs would be a great step towards promoting a deeper understanding of how these three-dimensional frameworks are formed and how to produce targeted topologies.

ii) Implementation of *in situ* X-ray diffraction (XRD) experiments. As shown in various studies, particularly in the field of protein crystallization [59–62], it is possible to couple microfluidic devices and automated X-ray analysis both in laboratory diffractometers [63] and at large-scale synchrotron facilities [64]. The crystalline nature of COFs makes the adaptation and implementation of these technologies for the *in situ* study of both crystal structures and the kinetics of crystal formation and growth a desirable goal. This would comprise the study of COFs generated by either continuous or segmented-flow approaches, with the aim at conducting *in situ* X-ray diffraction experiments (including single-crystal XRD (SC-XRD), powder XRD (PXRD), and SAXS experiments) to gain new mechanistic insights on the main features directing the formation and growth of COFs.

iii) Besides the design of devices for the synthesis and processing of COFs, special attention should be focused on parallelisation and/or automation of these methods. The continuous flow processes described here work with small volumes, but the effective footprint of each reactor is much smaller than conventional synthesis equipment. In order to make these methods viable in an industrial setting, the number of devices performing the same syntheses needs to be increased and these new experimental setups optimised.

iv) Coupling of microfluidic technologies with 3D printing. An alternative way of enhancing the processability of COFs by using direct-ink writing (DIW) 3D printing has been reported by some research groups [57,58,65]. In these approaches, the COFs are synthesised inside a fluid matrix of adequate rheological properties and then extruded to form 3D monoliths of various characteristics. These studies show that it is possible to form structures with functional shapes and with one or more COF domains incorporated. If these processes are adapted to be compatible with microfluidic conditions, it should be possible to obtain functional 3D COF materials and the need for binder formulations during the printing process could be avoided.

Declaration of Competing Interest

The authors declare that they have no known competing financial interests or personal relationships that could have appeared to influence the work reported in this paper.

Acknowledgements

This work is supported by the European Research Council Starting Grant microCryFact (ERC-2015-STG No. 677020), the Swiss National Science Foundation (project no. 200021_181988), and grant PID2020-116612RB-C33 funded by MCIN/AEI/10.13039/501100011033. S.P. acknowledges support from the ERC-2017-CoG HINBOTS Grant No. 771565.

References

- [1] A.P. Côté, A.I. Benin, N.W. Ockwig, M. O’Keeffe, A.J. Matzger, O.M. Yaghi, Chemistry: Porous, crystalline, covalent organic frameworks, *Science*. 310 (2005) 1166–1170, <https://doi.org/10.1126/science.1120411>.
- [2] R. Freund, S. Canossa, S.M. Cohen, W. Yan, H. Deng, V. Guillermin, M. Eddaoudi, D. G. Madden, D. Fairen-Jimenez, H. Lyu, L.K. Macreadie, Z. Ji, Y. Zhang, B. Wang, F. Haase, C. Wöll, O. Zaremba, J. Andreo, S. Wuttke, C.S. Diercks, 25 Years of Reticular Chemistry, *Angew. Chemie Int. Ed.* 60 (45) (2021) 23946–23974, <https://doi.org/10.1002/anie.202101644>.
- [3] H. Li, A.D. Chavez, H. Li, H. Li, W.R. Dichtel, J.-L. Bredas, Nucleation and Growth of Covalent Organic Frameworks from Solution: The Example of COF-5, *J. Am. Chem. Soc.* 139 (45) (2017) 16310–16318, <https://doi.org/10.1021/jacs.7b09169>.
- [4] C. Feriante, A.M. Evans, S. Jhuulki, I. Castano, M.J. Strauss, S. Barlow, W.R. Dichtel, S.R. Marder, New mechanistic insights into the formation of imine-linked two-dimensional covalent organic frameworks, *J. Am. Chem. Soc.* 142 (43) (2020) 18637–18644, <https://doi.org/10.1021/jacs.0c08390>.
- [5] G.A. Ozin, Morphogenesis of Biomineral and Morphosynthesis of Biomimetic Forms, *Acc. Chem. Res.* 30 (1) (1997) 17–27, <https://doi.org/10.1021/ar960021r>.
- [6] O.M. Yaghi, M.J. Kalmutzki, C.S. Diercks, Introduction to reticular chemistry: Metal-organic frameworks and covalent organic frameworks (2019), <https://doi.org/10.1002/9783527821099>.
- [7] F. Haase, B.V. Lotsch, Solving the COF trilemma: Towards crystalline, stable and functional covalent organic frameworks, *Chem. Soc. Rev.* 49 (23) (2020) 8469–8500, <https://doi.org/10.1039/D0CS01027H>.
- [8] X. Chen, L. Xia, R. Pan, X. Liu, Covalent organic framework mesocrystals through dynamic modulator manipulated mesoscale self-assembly of imine macrocycle precursors, *J. Colloid Interface Sci.* 568 (2020) 76–80, <https://doi.org/10.1016/j.jcis.2020.02.046>.
- [9] S. Sevim, A. Sorrenti, C. Franco, S. Furukawa, S. Pané, A.J. deMello, J. Puigmartí-Luis, Self-assembled materials and supramolecular chemistry within microfluidic environments: From common thermodynamic states to non-equilibrium structures, *Chem. Soc. Rev.* 47 (11) (2018) 3788–3803, <https://doi.org/10.1039/C8CS00025E>.
- [10] A. Sorrenti, J. Leira-Iglesias, A.J. Markvoort, T.F.A. de Greef, T.M. Hermans, Non-equilibrium supramolecular polymerization, *Chem. Soc. Rev.* 46 (18) (2017) 5476–5490, <https://doi.org/10.1039/C7CS00121E>.
- [11] B.A. Grzybowski, *Chemistry in Motion: Reaction-Diffusion Systems for Micro- and Nanotechnology*, Wiley, 2009.
- [12] A. Sorrenti, R. Rodríguez-Trujillo, D.B. Amabilino, J. Puigmartí-Luis, Milliseconds Make the Difference in the Far-from-Equilibrium Self-Assembly of Supramolecular Chiral Nanostructures, *J. Am. Chem. Soc.* 138 (22) (2016) 6920–6923, <https://doi.org/10.1021/jacs.6b02538>.
- [13] M. Rubio-Martínez, I. Imaz, N. Domingo, A. Abrishamkar, T.S. Mayor, R.M. Rossi, C. Carbonell, A.J. deMello, D.B. Amabilino, D. Maspoch, J. Puigmartí-Luis, Freezing the Nonclassical Crystal Growth of a Coordination Polymer Using Controlled Dynamic Gradients, *Adv. Mater.* 28 (37) (2016) 8150–8155, <https://doi.org/10.1002/adma.201506462>.
- [14] Y. Zhao, Z. Liao, Z. Xiang, Microfluidics for synthesis and morphology control of hierarchical porous covalent organic polymer monolith, *Chem. Eng. Sci.* 195 (2019) 801–809, <https://doi.org/10.1016/j.ces.2018.10.026>.
- [15] Y. Xin, S. Peng, J. Chen, Z. Yang, J. Zhang, Continuous flow synthesis of porous materials, *Chinese Chem. Lett.* 31 (6) (2020) 1448–1461, <https://doi.org/10.1016/j.ccl.2019.09.054>.
- [16] A.-G. Niculescu, C. Chircov, A.C. Bîrcă, A.M. Grumezescu, Nanomaterials Synthesis through Microfluidic Methods: An Updated Overview, *Nanomaterials*. 11 (2021) 864, <https://doi.org/10.3390/nano11040864>.
- [17] Y. Dou, B. Wang, M. Jin, Y. Yu, G. Zhou, L. Shui, A review on self-assembly in microfluidic devices, *J. Micromech. Microeng.* 27 (11) (2017) 113002, <https://doi.org/10.1088/1361-6439/aa84db>.
- [18] L. Wang, S. Sánchez, Self-assembly via microfluidics, *Lab Chip*. 15 (23) (2015) 4383–4386, <https://doi.org/10.1039/C5LC90116B>.
- [19] C. Hu, Y. Bai, M. Hou, Y. Wang, L. Wang, X. Cao, C.-W. Chan, H. Sun, W. Li, J. Ge, K. Ren, Defect-induced activity enhancement of enzyme-encapsulated metal-organic frameworks revealed in microfluidic gradient mixing synthesis, *Sci. Adv.* 6 (5) (2020), <https://doi.org/10.1126/sciadv.aax5785>.
- [20] M. Faustini, J. Kim, G.-Y. Jeong, J.Y. Kim, H.R. Moon, W.-S. Ahn, D.-P. Kim, Microfluidic approach toward continuous and ultrafast synthesis of metal-organic framework crystals and hetero structures in confined microdroplets, *J. Am. Chem. Soc.* 135 (39) (2013) 14619–14626, <https://doi.org/10.1021/ja4039642>.
- [21] M. Sultana, K.F. Jensen, Microfluidic continuous seeded crystallization: Extraction of growth kinetics and impact of impurity on morphology, *Cryst. Growth Des.* 12 (12) (2012) 6260–6266, <https://doi.org/10.1021/cg301538y>.
- [22] M. Ildefonso, N. Candoni, S. Veessler, Using microfluidics for fast, accurate measurement of lysozyme nucleation kinetics, *Cryst. Growth Des.* 11 (5) (2011) 1527–1530, <https://doi.org/10.1021/cg101431g>.
- [23] N. Calvo Galve, A. Abrishamkar, A. Sorrenti, L. Di Rienzo, M. Satta, M. D’Abramo, E. Coronado, A.J. Mello, G. Mínguez Espallargas, J. Puigmartí-Luis, Exploiting Reaction-Diffusion Conditions to Trigger Pathway Complexity in the Growth of a MOF, *Angew. Chemie – Int. Ed.* 60 (29) (2021) 15920–15927, <https://doi.org/10.1002/anie.202101611>.
- [24] J. Puigmartí-Luis, M. Rubio-Martínez, U. Hartfelder, I. Imaz, D. Maspoch, P. S. Dittrich, Coordination polymer nanofibers generated by microfluidic synthesis, *J. Am. Chem. Soc.* 133 (12) (2011) 4216–4219, <https://doi.org/10.1021/ja110834j>.

- [25] A. Sorrenti, L. Jones, S. Sevim, X. Cao, A.J. deMello, C. Martí-Gastaldo, J. Puigmartí-Luis, Growing and Shaping Metal-Organic Framework Single Crystals at the Millimeter Scale, *J. Am. Chem. Soc.* 142 (20) (2020) 9372–9381, <https://doi.org/10.1021/jacs.0c01935>.
- [26] C. Echaide-Górriz, C. Clément, F. Cacho-Bailo, C. Téllez, J. Coronas, New strategies based on microfluidics for the synthesis of metal-organic frameworks and their membranes, *J. Mater. Chem. A*. 6 (14) (2018) 5485–5506, <https://doi.org/10.1039/C8TA01232F>.
- [27] M. Solsona, J.C. Vollenbroek, C.B.M. Tregouet, A.-E. Nieuwelink, W. Olthuis, A. van den Berg, B.M. Weckhuysen, M. Odijk, Microfluidics and catalyst particles, *Lab Chip*. 19 (21) (2019) 3575–3601, <https://doi.org/10.1039/C9LC000318E>.
- [28] Y. Tanaka, S. Yamada, D. Tanaka, Continuous Fluidic Techniques for the Precise Synthesis of Metal-Organic Frameworks, *Chempluschem*. 86 (4) (2021) 650–661, <https://doi.org/10.1002/cplu.202000798>.
- [29] M. Gonidec, J. Puigmartí-Luis, Continuous- versus segmented-flow microfluidic synthesis in materials science, *Crystals*. 9 (2019) 12, <https://doi.org/10.3390/cryst9010012>.
- [30] J.B. Knight, A. Vishwanath, J.P. Brody, R.H. Austin, Hydrodynamic focusing on a silicon chip: Mixing nanoliters in microseconds, *Phys. Rev. Lett.* 80 (17) (1998) 3863–3866, <https://doi.org/10.1103/PhysRevLett.80.3863>.
- [31] J. Puigmartí-Luis, D. Schaffhauser, B.R. Burg, P.S. Dittrich, A microfluidic approach for the formation of conductive nanowires and hollow hybrid structures, *Adv. Mater.* 22 (20) (2010) 2255–2259, <https://doi.org/10.1002/adma.200903428>.
- [32] A. Abrishamkar, S. Suárez-García, S. Sevim, A. Sorrenti, R. Pons, S.-X. Liu, S. Decurtins, G. Aromí, D. Aguilà, S. Pané, A.J. deMello, A. Rotaru, D. Ruiz-Molina, J. Puigmartí-Luis, Pathway selection as a tool for crystal defect engineering: A case study with a functional coordination polymer, *Appl. Mater. Today*. 20 (2020) 100632, <https://doi.org/10.1016/j.apmt.2020.100632>.
- [33] R.B. Bird, W.E. Stewart, E.N. Lightfoot, *Transport Phenomena*, Second Edi, John Wiley and Sons Inc., 2002.
- [34] A. Vergara, B. Lorber, A. Zagari, R. Giegé, Physical aspects of protein crystal growth investigated with the advanced protein crystallization facility in reduced-gravity environments, *Acta Crystallogr. – Sect. D Biol. Crystallogr.* 59 (1) (2003) 2–15, <https://doi.org/10.1107/S0907444902021443>.
- [35] S. Mann, *Biomaterialization: Principles and Concepts in Bioinorganic Materials Chemistry*, Oxford University Press, 2001.
- [36] D. Rodríguez-San-Miguel, F. Zamora, Processing of covalent organic frameworks: An ingredient for a material to succeed, *Chem. Soc. Rev.* 48 (16) (2019) 4375–4386, <https://doi.org/10.1039/C9CS00258H>.
- [37] D. Rodríguez-San-Miguel, A. Abrishamkar, J.A.R. Navarro, R. Rodríguez-Trujillo, D.B. Amabilino, R. Mas-Ballesté, F. Zamora, J. Puigmartí-Luis, Crystalline fibres of a covalent organic framework through bottom-up microfluidic synthesis, *Chem. Commun.* 52 (59) (2016) 9212–9215, <https://doi.org/10.1039/C6CC04013F>.
- [38] A. Abrishamkar, D. Rodríguez-San-Miguel, J.A. Rodríguez Navarro, R. Rodríguez-Trujillo, D.B. Amabilino, R. Mas-Ballesté, F. Zamora, A.J. deMello, J. Puigmartí-Luis, Microfluidic-based synthesis of covalent organic frameworks (COFs): A tool for continuous production of COF fibers and direct printing on a surface, *J. Vis. Exp.* 2017 (2017) 1–8, <https://doi.org/10.3791/56020>.
- [39] Y. Peng, W.K. Wong, Z. Hu, Y. Cheng, D. Yuan, S.A. Khan, D. Zhao, Room Temperature Batch and Continuous Flow Synthesis of Water-Stable Covalent Organic Frameworks (COFs), *Chem. Mater.* 28 (14) (2016) 5095–5101, <https://doi.org/10.1021/acs.chemmater.6b01954>.
- [40] N. Nivedita, P. Ligrani, I. Papatouky, Dean Flow Dynamics in Low-Aspect Ratio Spiral Microchannels, *Sci. Rep.* 7 (2017) 1–10, <https://doi.org/10.1038/srep44072>.
- [41] R.P. Bisbey, C.R. DeBlase, B.J. Smith, W.R. Dichtel, Two-dimensional Covalent Organic Framework Thin Films Grown in Flow, *J. Am. Chem. Soc.* 138 (36) (2016) 11433–11436, <https://doi.org/10.1021/jacs.6b04669>.
- [42] V. Singh, S. Jang, N.K. Vishwakarma, D.-P. Kim, Intensified synthesis and post-synthetic modification of covalent organic frameworks using a continuous flow of microdroplets technique, *NPG Asia Mater.* 10 (1) (2018) e456, <https://doi.org/10.1038/am.2017.209>.
- [43] M. Liu, X.-P. Chen, Numerical study on the stick-slip motion of contact line moving on heterogeneous surfaces, *Phys. Fluids*. 29 (8) (2017) 082102, <https://doi.org/10.1063/1.4996189>.
- [44] A. McPherson, L.J. DeLucas, Microgravity protein crystallization, *Npj Microgravity* 11 (1) (2015) 1–20, <https://doi.org/10.1038/npjmgrav.2015.10>.
- [45] C.E. Kundrot, R.A. Judge, M.L. Pusey, E.H. Snell, Microgravity and macromolecular crystallography, *Cryst. Growth Des.* 1 (1) (2001) 87–99, <https://doi.org/10.1021/cg005511b>.
- [46] R.L. Kroes, D. Reiss, Properties of TGS aqueous solution for crystal growth, *J. Cryst. Growth*. 69 (2-3) (1984) 414–420, [https://doi.org/10.1016/0022-0248\(84\)90351-8](https://doi.org/10.1016/0022-0248(84)90351-8).
- [47] M.D. Aggarwal, A.K. Batra, R.B. Lal, B.G. Penn, D.O. Frazier, Bulk Single Crystals Grown from Solution on Earth and in Microgravity, *Springer Handb. Cryst. Growth*. (2010) 559–598, https://doi.org/10.1007/978-3-540-74761-1_17.
- [48] S. Koszelak, J. Day, C. Leja, R. Cudney, A. McPherson, Protein and Virus Crystal Growth on International Microgravity Laboratory-2, *Biophys. J.* 69 (1) (1995) 13–19, [https://doi.org/10.1016/S0006-3495\(95\)79890-3](https://doi.org/10.1016/S0006-3495(95)79890-3).
- [49] I. Cozmata, D.J. Rasky, Exotic Optical Fibers and Glasses: Innovative Material Processing Opportunities in Earth's Orbit, *New Sp. J.* 5 (3) (2017) 121–140, <https://doi.org/10.1089/space.2017.0016>.
- [50] A.K. Gangopadhyay, M.E. Sellers, G.P. Bracker, D. Holland-Moritz, D.C. Van Hoesen, S. Koch, P.K. Galenko, A.K. Pauls, R.W. Hyers, K.F. Kelton, Demonstration of the effect of stirring on nucleation from experiments on the International Space Station using the ISS-EML facility, *npj Microgravity* 7 (2021) 1–6, <https://doi.org/10.1038/s41526-021-00161-9>.
- [51] H. Ahari, R.L. Bedard, C.L. Bowes, N. Coombs, O. Dag, T. Jiang, G.A. Ozin, S. Petrov, I. Sokolov, A. Verma, G. Vovk, D. Young, Effect of microgravity on the crystallization of a self-assembling layered material, *Nature* 388 (6645) (1997) 857–860, <https://doi.org/10.1038/42213>.
- [52] H. Nguyen-Thi, G. Reinhart, B. Billia, On the interest of microgravity experimentation for studying convective effects during the directional solidification of metal alloys, *Comptes Rendus – Mec.* 345 (1) (2017) 66–77, <https://doi.org/10.1016/j.crme.2016.10.007>.
- [53] J.M. Alford, G.R. Mason, D.A. Feikema, Formation of Carbon Nanotubes in a Microgravity Environment, in: *Sixth Int. Microgravity Combust. Work*, 2001.
- [54] A. Zocca, J. Lichtenborg, T. Mühler, J. Wilbig, G. Mohr, T. Villatte, F. Léonard, G. Nolze, M. Sparenberg, J. Melcher, K. Hilgenberg, J. Günster, Enabling the 3D Printing of Metal Components in μ -Gravity, *Adv. Mater. Technol.* 4 (10) (2019) 1900506, <https://doi.org/10.1002/admt.201900506>.
- [55] N. Contreras-Pereda, D. Rodríguez-San-Miguel, C. Franco, S. Sevim, J.P. Vale, E. Solano, W.-K. Fong, A. Del Giudice, L. Galantini, R. Pfattner, S. Pané, T.S. Mayor, D. Ruiz-Molina, J. Puigmartí-Luis, Synthesis of 2D Porous Crystalline Materials in Simulated Microgravity, *Adv. Mater.* 33 (30) (2021) 2101777, <https://doi.org/10.1002/adma.202101777>.
- [56] C. Franco, D. Rodríguez-San-Miguel, A. Sorrenti, S. Sevim, R. Pons, A.E. Platero-Prats, M. Pavlovic, I. Szilágyi, M.L. Ruiz Gonzalez, J.M. González-Calbet, D. Bochicchio, L. Pesce, G.M. Pavan, I. Imaz, M. Cano-Sarabia, D. Maspocho, S. Pané, A.J. de Mello, F. Zamora, J. Puigmartí-Luis, Biomimetic Synthesis of Sub-20 nm Covalent Organic Frameworks in Water, *J. Am. Chem. Soc.* 142 (7) (2020) 3540–3547, <https://doi.org/10.1021/jacs.9b12389>.
- [57] A.K. Mohammed, S. Usgaonkar, F. Kanheerampockil, S. Karak, A. Halder, M. Tharkar, M. Addicoat, T.G. Ajithkumar, R. Banerjee, Connecting Microscopic Structures, Mesoscale Assemblies, and Macroscopic Architectures in 3D-Printed Hierarchical Porous Covalent Organic Framework Foams, *J. Am. Chem. Soc.* 142 (18) (2020) 8252–8261, <https://doi.org/10.1021/jacs.0c00555>.
- [58] M. Zhang, L. Li, Q. Lin, M. Tang, Y. Wu, C. Ke, Hierarchical-Coassembly-Enabled 3D-Printing of Homogeneous and Heterogeneous Covalent Organic Frameworks, *J. Am. Chem. Soc.* 141 (13) (2019) 5154–5158, <https://doi.org/10.1021/jacs.9b01561>.
- [59] C.L. Hansen, E. Skordalakes, J.M. Berger, S.R. Quake, A robust and scalable microfluidic metering method that allows protein crystal growth by free interface diffusion, *Proc. Natl. Acad. Sci.* 99 (26) (2002) 16531–16536, <https://doi.org/10.1073/pnas.262485199>.
- [60] S. Guha, S.L. Perry, A.S. Pawate, P.J.A. Kenis, Fabrication of X-ray compatible microfluidic platforms for protein crystallization, *Sensors Actuat., B Chem.* 174 (2012) 1–9, <https://doi.org/10.1016/j.snb.2012.08.048>.
- [61] N. Junius, S. Jaho, Y. Sallaz-Damaz, F. Borel, J.-B. Salmon, M. Budayova-Spano, A microfluidic device for both on-chip dialysis protein crystallization and in situ X-ray diffraction, *Lab Chip*. 20 (2) (2020) 296–310, <https://doi.org/10.1039/C9LC00651F>.
- [62] A. Ghazal, J.P. Lafleur, K. Mortensen, J.P. Kutter, L. Arleth, G.V. Jensen, Recent advances in X-ray compatible microfluidics for applications in soft materials and life sciences, *Lab Chip*. 16 (22) (2016) 4263–4295, <https://doi.org/10.1039/C6LC00888G>.
- [63] XtalCheck-S|Automated in situ X-ray crystallography, (n.d.). <https://www.rigaku.com/products/crystallography/xtalcheck> (accessed August 31, 2021).
- [64] I. Chaussovoine, A. Beauvois, T. Mateo, R. Vasireddi, N. Douri, J. Priam, Y. Liatimi, S. Lefrançois, H. Tabuteau, M. Davranche, D. Vantelon, T. Bizien, L.M.G. Chavas, B. Lassalle-Kaiser, The microfluidic laboratory at Synchrotron SOLEIL, *J. Synchrotron Radiat.* 27 (1) (2020) 230–237, <https://doi.org/10.1107/S1600577519015042>.
- [65] X. Liu, G.J.H. Lim, Y. Wang, L. Zhang, D. Mullangi, Y. Wu, D. Zhao, J. Ding, A. K. Cheetham, J. Wang, Binder-free 3D printing of covalent organic framework (COF) monoliths for CO₂ adsorption, *Chem. Eng. J.* 403 (2021) 126333, <https://doi.org/10.1016/j.cej.2020.126333>.